# Differential cross sections in the ejected energy for an $L=0$ model of the electron-impact ionization of hydrogen

M. S. Pindzola and F. Robicheaux
*Department of Physics, Auburn University, Auburn, Alabama 36849*
(Received 25 November 1996)

A calculational procedure is formulated for extracting differential cross sections in the ejected energy from a time-dependent wave-packet method for the electron ionization of hydrogen. The procedure is applied to an $s$-wave model for electron-hydrogen scattering. In contrast to recent time-independent methods, the differential cross sections are found to be smooth and symmetric. [S1050-2947(97)08706-4]

PACS number(s): 34.80.Dp

In the last year a time-dependent wave-packet method has been employed to calculate the total cross section for the electron-impact ionization of hydrogen [1,2]. The time-dependent results are in excellent agreement with both experimental measurements [3] and recent time-independent close-coupling calculations [4–6]. In this paper we formulate a calculational procedure for extracting differential cross sections in the ejected energy from the time-dependent wave-packet method. The formulation is based on an extension of an idea by Bottcher [7]. We then apply the procedure to calculate singlet and triplet differential cross sections for the Temkin-Poet model [8,9] of electron-hydrogen scattering. The specific application is in response to discrepancies found between two different time-independent close-coupling calculations for the singlet differential cross section [10].

The time-dependent Schrodinger equation for the Temkin-Poet model is given by (in atomic units)

$$i\,\frac{\partial\psi(r_1,r_2,t)}{\partial t}=H(r_1,r_2)\,\psi(r_1,r_2,t), \tag{1}$$

where the time-independent Hamiltonian is

$$H(r_1,r_2)=-\frac{1}{2}\,\frac{\partial^2}{\partial r_1^2}-\frac{1}{2}\,\frac{\partial^2}{\partial r_2^2}-\frac{1}{r_1}-\frac{1}{r_2}+\frac{1}{r_>}, \tag{2}$$

and $r_>=\max(r_1,r_2)$. We solve this time-dependent equation on a two-dimensional lattice using an explicit leapfrog propagator [2]. At time $t=0$ the wave function is constructed as a symmetric product of an incoming radial wave packet for one electron and the lowest-energy bound stationary state of the other electron. Cross sections may be extracted from the wave function at a time $t=T$ following the collision. The $(r_1,r_2)$ plane may be divided into angular segments specified by the hyperspherical angle $\alpha$, where $\tan(\alpha)=(r_2/r_1)$. The differential cross section in the hyperspherical angle is given by [7]:

$$\frac{d\sigma}{d\alpha}=\frac{\pi(2S+1)}{4k_0^2}\lim_{\delta\to 0}\frac{1}{\delta}\int_{\alpha-(\delta/2)}^{\alpha+(\delta/2)}|\psi(r_1,r_2,T)|^2\,dr_1\,dr_2, \tag{3}$$

where $S$ is the total spin angular momentum and $k_0$ is the linear momentum of the incident electron. Since in the long-time limit we also have $\tan(\alpha)=(k_2/k_1)$, where $k_1$ and $k_2$ are the outgoing linear momenta of the two electrons following ionization, the differential cross section in ejected energy is given by

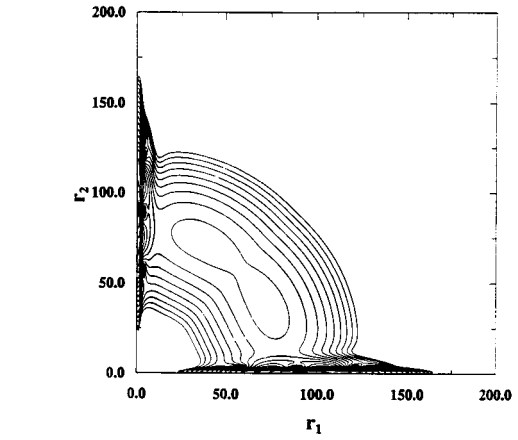


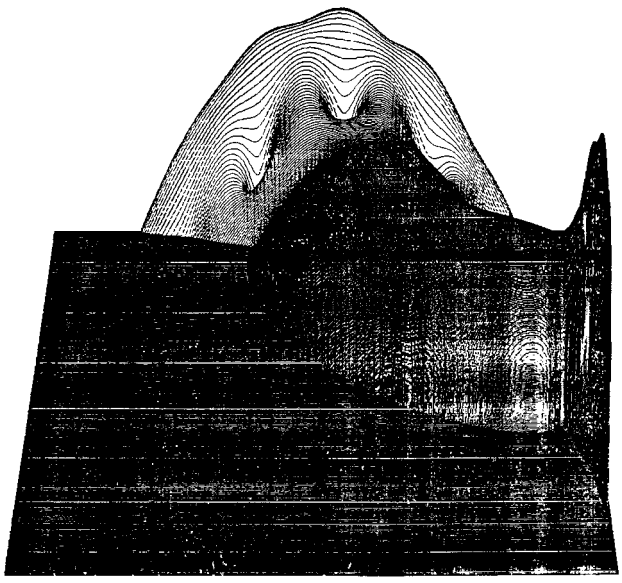

FIG. 1. Probability density $|\psi(r_1,r_2,T)|^2$ following a $^1S$ collision at 54.4 eV. At the top is a contour map in the $(r_1,r_2)$ plane, while the bottom is the corresponding 3D projection. The radial coordinates are in atomic units (1 a.u.$=5.29\times10^{-9}$ cm).

 

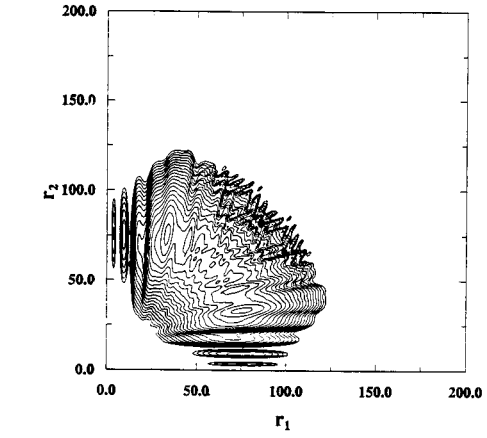


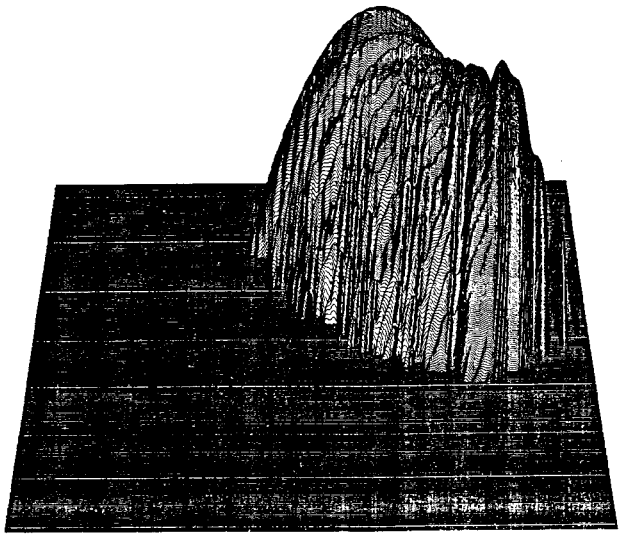

FIG. 2. Probability density $|Q\psi(r_1,r_2,T)|^2$ following a $^1S$ collision at 54.4 eV. At the top is a contour map in the $(r_1,r_2)$ plane, while the bottom is the corresponding 3D projection. The radial coordinates are in atomic units (1 a.u.$=5.29\times10^{-9}$ cm).

$$\frac{d\sigma}{d\epsilon}=\frac{1}{k_1k_2}\frac{d\sigma}{d\alpha}, \tag{4}$$

*where* $\epsilon=k_2^2/2, E=(k_0^2/2)+I_p=(k_1^2/2+(k_2^2/2)$ *is the total energy, and* $I_p$ *is the ionization potential of the target.*

To make accurate calculations of the differential cross section for small ($\alpha\sim0$) and large ($\alpha\sim\pi/2$) angles, we choose to replace the total wave function $\psi(r_1,r_2,T)$ found in Eq. (3) by a pure double-continuum wave function $Q\psi(r_1,r_2,T)$. The projection operator $Q$ needed to extract only the double-continuum part of the total time evolved wave function is given by

$$Q=1-\sum_n |P_n(r_1)\rangle\langle P_n(r_1)|-\sum_n |P_n(r_2)\rangle\langle P_n(r_2)|$$

$$+\sum_m\sum_n |P_m(r_1)P_n(r_2)\rangle\langle P_m(r_1)P_n(r_2)|. \tag{5}$$

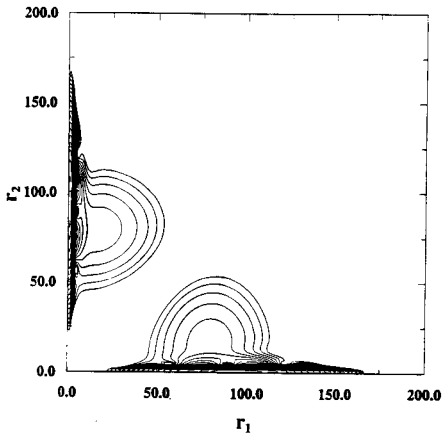


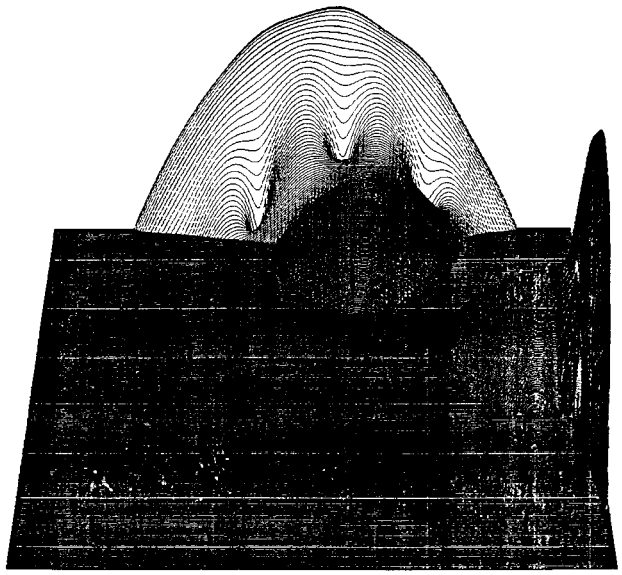

FIG. 3. Probability density $|\psi(r_1,r_2,T)|^2$ following a $^3S$ collision at 54.4 eV. At the top is a contour map in the $(r_1,r_2)$ plane, while the bottom is the corresponding 3D projection. The radial coordinates are in atomic units (1 a.u.$=5.29\times10^{-9}$ cm).

This projection operator is constructed so that $Q\psi$ is a function of $(r_1,r_2)$, in which neither electron is in a bound state. The single-particle bound eigenfunctions $P_n(r)$ are obtained by diagonalizing $h(r)=-\frac{1}{2}(\partial^2/\partial r^2)-(1/r)$ on a one-dimensional lattice. In practice, the double bound-state term on the right-hand side of Eq. (5) makes little contribution.

The dramatic effect of the projection operator is illustrated by comparing Figs. 1 and 2. We employ a $10^6$ point lattice with a uniform mesh spacing in both $r_1$ and $r_2$ of $\Delta r=0.2$, which corresponds to a box size of $R=200$. At time $t=0$ the symmetric $^1S$ wave packet is centered at $R/2=100$. At time $t=T=100$, following a collision with an incident electron energy of 54.4 eV (velocity $=2.0$), the total probability density $|\psi(r_1,r_2,T)|^2$ is shown as a contour map and a three-dimensional (3D) projection in Fig. 1. In sharp contrast the total probability density $|Q\psi(r_1,r_2,T)|^2$ is shown in Fig. 2. In the figures the probability density is moving toward the upper right-hand corner in the contour map, and toward the lower left-hand corner in the 3D pro-

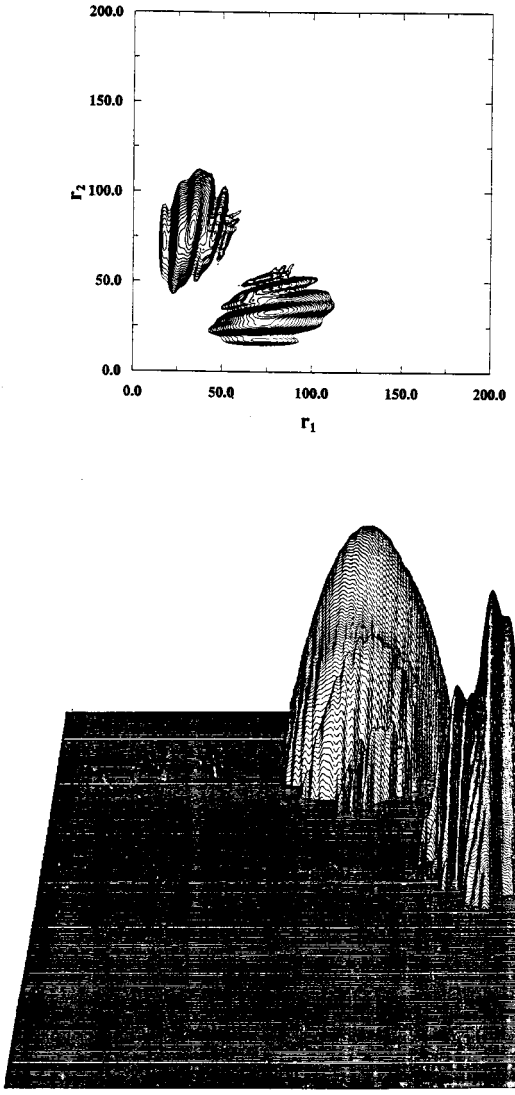


FIG. 4. Probability density $|Q\psi(r_1,r_2,T)|^2$ following a $^3S$ collision at 54.4 eV. At the top is a contour map in the $(r_1,r_2)$ plane, while the bottom is the corresponding 3D projection. The radial coordinates are in atomic units (1 a.u.$=5.29\times10^{-9}$ cm).

jection as a function of increasing time after the collision. Essentially the large peaks along the axes, representing elastic scattering and inelastic excitation to bound states, have been eliminated. Note that the contours have been rescaled between the figures so that absolute heights cannot be compared. For the same scattering parameters, the effect of the projection operator on the antisymmetric $^3S$ wave packet is found by comparing Figs. 3 and 4.

The singlet and triplet differential cross sections in the Temkin-Poet model of electron-hydrogen scattering are shown in Figs. 5 and 6 for an incident electron energy of 54.4 eV. The five lines in each figure represent five successive calculations on larger lattices. The mesh spacing is kept fixed at $\Delta r=0.2$, while the box size is increased from $R=100$ to 500 in steps of 100. For singlet scattering the total ionization cross section is found to be the same value of 1.38 Mb for each successive calculation, while for triplet scattering the total cross section is a constant 0.30 Mb. The continual spreading of the cross-section peaks is due to the long-range Coulomb interaction. The center of the distribution

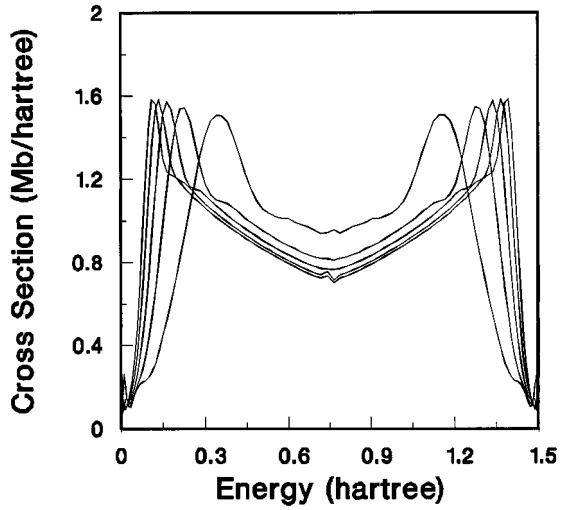


FIG. 5. Singlet differential cross section in the ejected energy for a collision at 54.4 eV. The five lines are successive calculations at larger box sizes. 1 Mb is $10^{-18}$ cm$^2$ and 1 hartree is 27.212 eV.

represents an equal energy sharing of the outgoing electrons, finite for singlet scattering, but zero for triplet scattering. The peaks of the distribution represent the ejection of one slow electron and one fast electron. The fast electron sees a neutral atom, while the slow electron ''feels'' a $-1/r$ attractive Coulomb potential. Although the fast electron may be out near the box radius, the slow electron is in closer, and still feels a sizeable force. As $R\rightarrow\infty$ the cross section peaks will merge into the walls of the figures to yield symmetric curves with no structure.

Recently two different close-coupling calculations have reported [10] singlet and triplet differential ionization cross sections for the Temkin-Poet model at an incident energy of 54.4 eV. Both the $R$-matrix with pseudostates method and the converged close-coupling method are time-independent scattering treatments utilizing explicit boundary conditions to extract the $S$ matrix and thus cross sections. The time-dependent wave packet and time independent close-coupling calculations are in agreement as to the total ionization cross

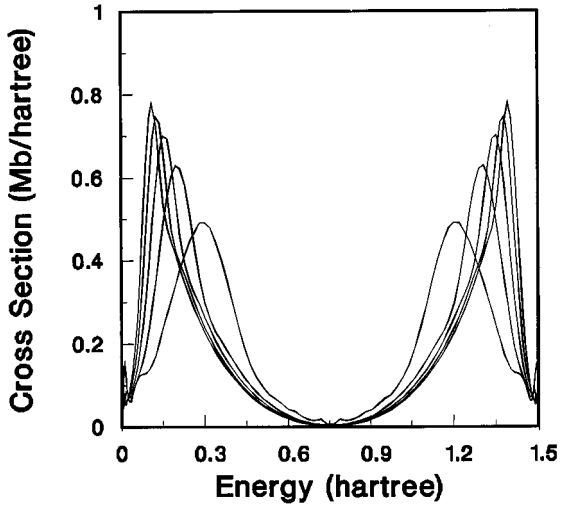


FIG. 6. Triplet differential cross section in the ejected energy for a collision at 54.4 eV. The five lines are successive calculations at larger box sizes. 1 Mb is $10^{-18}$ cm$^2$ and 1 hartree is 27.212 eV.

sections for singlet and triplet scattering. At least in the current formulations, the time-independent close-coupling methods produce asymmetric differential cross sections, which go to zero for energies greater than $E/2$. This is in sharp contrast to the symmetric results found in Figs. 5 and 6 for the time-dependent wave-packet method. The discrepancies found between the two time-independent close-coupling calculations for the singlet differential cross section, and the report of remarkable structure, may be due to an unphysical cutoff of the nonzero cross section at $E/2$.

In summary we have made use of a projection operator to extract differential cross sections in the ejected energy for a time-dependent wave-packet method for electron-atom scattering. The wave function $Q\psi$ represents the double-electron continuum and may be graphically displayed in the $(r_1, r_2)$ plane as found in Figs. 2 and 4. The differential cross sections obtained using $Q\psi$ are found to be smooth and symmetric about $E/2$, in contrast to recent results from time-independent close-coupling methods. In the future we plan to extend our differential cross-section calculations to lower incident energies to gain further insight into the threshold law for the electron ionization of atoms.

We would like to thank Dr. Igor Bray of Flinders University for his encouraging us to examine the differential cross section in the ejected energy for the Temkin-Poet model. In this work, M.S.P. was supported in part by a NSF Grant (NSF-PHY-9122199) with Auburn University, and F.R. was supported in part by a NSF Young Investigator Grant (NSF-PHY-9457903) with Auburn University. Computational work was carried out at the National Energy Research Supercomputer Center in Livermore, California and the Center for Computational Sciences in Oak Ridge, Tennessee.

[1] M. S. Pindzola and D. R. Schultz, Phys. Rev. A **53**, 1525 (1996).
[2] M. S. Pindzola and F. Robicheaux, Phys. Rev. A **54**, 2142 (1996).
[3] M. B. Shah, D. S. Elliott, and H. B. Gilbody, J. Phys. B **20**, 3501 (1987).
[4] I. Bray and A. T. Stelbovics, Phys. Rev. Lett. **70**, 746 (1993).
[5] D. Kato and S. Watanabe, Phys. Rev. Lett. **74**, 2443 (1995).
[6] K. Bartschat and I. Bray, J. Phys. B **29**, L577 (1996).
[7] C. Bottcher, J. Phys. B. **14**, L349 (1981).
[8] A. Temkin, Phys. Rev. **126**, 130 (1962).
[9] R. Poet, J. Phys. B **11**, 3081 (1978).
[10] K. Bartschat and I. Bray, Phys. Rev. A **54**, R1002 (1996).